

Supporting Information.

Fig. S1. Domain architectures of T4CPs. T4CPs are composed of an N-terminal transmembrane domain (NTD), a nucleotide-binding domain (NBD), an all- α -domain (AAD), and in some cases a C-terminal domain (CTD). The schematics present domain structures of the TrwB_{R388} prototype and of T4CPs characterized in this study (listed at top). Upper: NTDs bearing two predicted transmembrane domains; residue numbers mark the boundaries of the membrane-spanning α -helices (gray cylinders). IM, inner membrane. Middle: Soluble domains composed of NBDs and AADs. At left, the solved structure of the TrwB_{R388} protomer lacking its NTD, with flanking residue numbers below. Predicted structures of corresponding regions of TraJ and VirD4 homologs determined by Phyre2 modeling; NBDs are multicolored, AADs are in green. Lower: CTD information. TrwB_{R388} and TraJ_{pKM101} lack CTDs. CTDs of the VirD4 homologs from *A. tumefaciens* (At), *A. phagocytophilum* (Ap), and *W. pipipientis* (Wp) vary in length and have a high proportion of acidic residues. CTD sequences are presented at the bottom; acidic Glu and Asp residues are in bold letters.

Fig. S2. Sequence alignments of T4CPs. Alignments of **A)** TraJ_{pKM101} with VirD4 subunits from *A. tumefaciens*, *A. phagocytophilum*, and *W. pipipientis*; **B)** TraJ_{pKM101} with TrwB_{R388}; **C)** VirD4 subunits from *A. tumefaciens*, *A. phagocytophilum*, and *W. pipipientis*; **D)** alphaproteobacterial VirD4 homologs with *L. pneumophila* DotL. Boxed regions denote N-terminal transmembrane domains (NTD), nucleotide binding domains and all- α -domains (NBD/AAD), and C-terminal domains (CTD). Red lettering, sequence identities; blue lettering, sequence similarities. **E)** Sequence alignments of the CTDs carried by VirD4 homologs from the *Wolbachia* species shown. Panel A: Schematic depiction showing variability in sequence lengths of the CTDs. Panel B: Sequence alignments of the CTDs showing variability in sequence compositions. Color scheme: Red, polar/acidic residues; Blue, polar/basic residues; Green, polar/neutral residues; Black, nonpolar residues.

Fig. S3. C-terminal sequences of known or candidate T4SS effectors. **A.** The *A. tumefaciens* effectors carry clusters of positively-charged Arg residues at their C termini. A systematic mutational analysis of VirF established the importance of Arg residues in an Arg(7x)Arg(x)Arg(xx)Arg motif (marked in red letters) for translocation through the *A. tumefaciens* VirB/VirD4 T4SS. A few Arg residues critical for VirF translocation are conserved near the C termini of *A. tumefaciens* VirE2 and VirE3, and one of these is also conserved among the *A. phagocytophilum* Ats-1 and the *W. pipipientis* WD0636, WD0811 and WalE1 effectors (red letters). The C termini of the effectors shown carry other positively-charged Arg or Lys residues (blue letters) and, notably, a high proportion of hydrophobic residues (underlined). Previous work identified clusters of hydrophobic residues at the C termini of effectors translocated through the *Legionella pneumophila* Dot/Icm T4SS, and a systematic mutational analysis established the importance of such residues for RalF translocation.

Fig. S4. Interactions of the VirE2CT100 fragment with VirD4_{At} domains as assessed by isothermal calorimetry (ITC). His₆-tagged VirE2CT100, MBP-tagged VirD4_{At} deleted of its N-terminal transmembrane domain and the AAD (designated NBD/CTD), and the MBP-tagged AAD_{VirD4At} were purified by sequential rounds of affinity chromatography and gel filtration chromatography using a Superose 6, 10/300 GL size exclusion column from GE Life Sciences. Binding of VirE2CT100 (185 μ M) to: **Panel A**, buffer alone; **Panel B**, the NBD/CTD variant; and **Panel C**, the AAD. Five microliter injections were used for each experiment, with 2 min between each injection to allow for peaks to reach baseline levels. The upper graphs show the raw data and the lower graphs show the normalized integration of the data. While apparent binding was observed in both **B** and **C**, low concentrations of NBD/CTD and AAD (higher concentrations could not be achieved due to aggregation) resulted in a low Wiseman “c” parameter, and could not be used to derive accurate thermodynamic information.

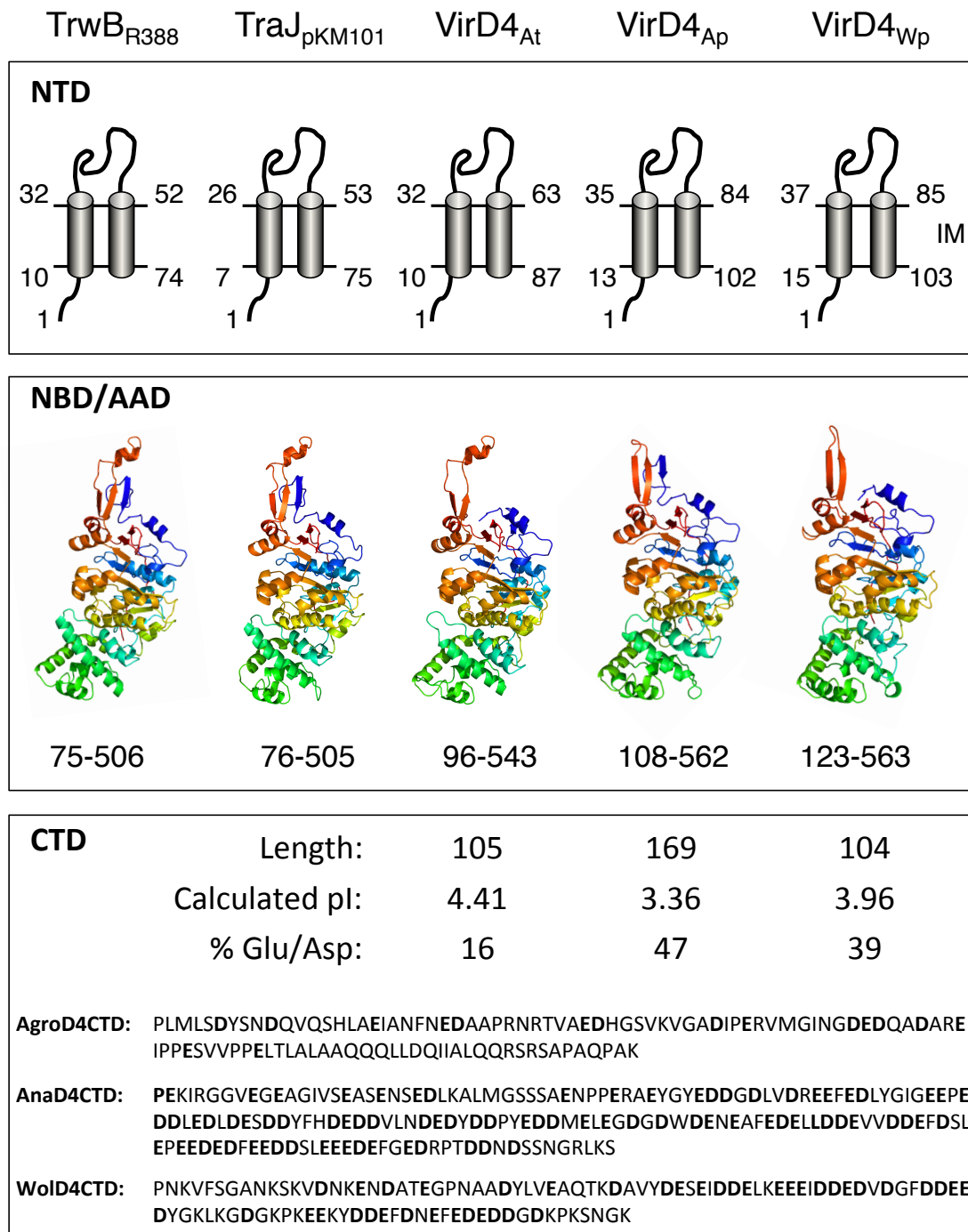


Fig. S1 Whitaker/Christie

Sequence Alignments of VirD4 Homologs

A

NTD

NBD/AAD

CTD

Fig. S2 Whitaker/Christie

B

Sequence Alignments of VirD4 Homologs

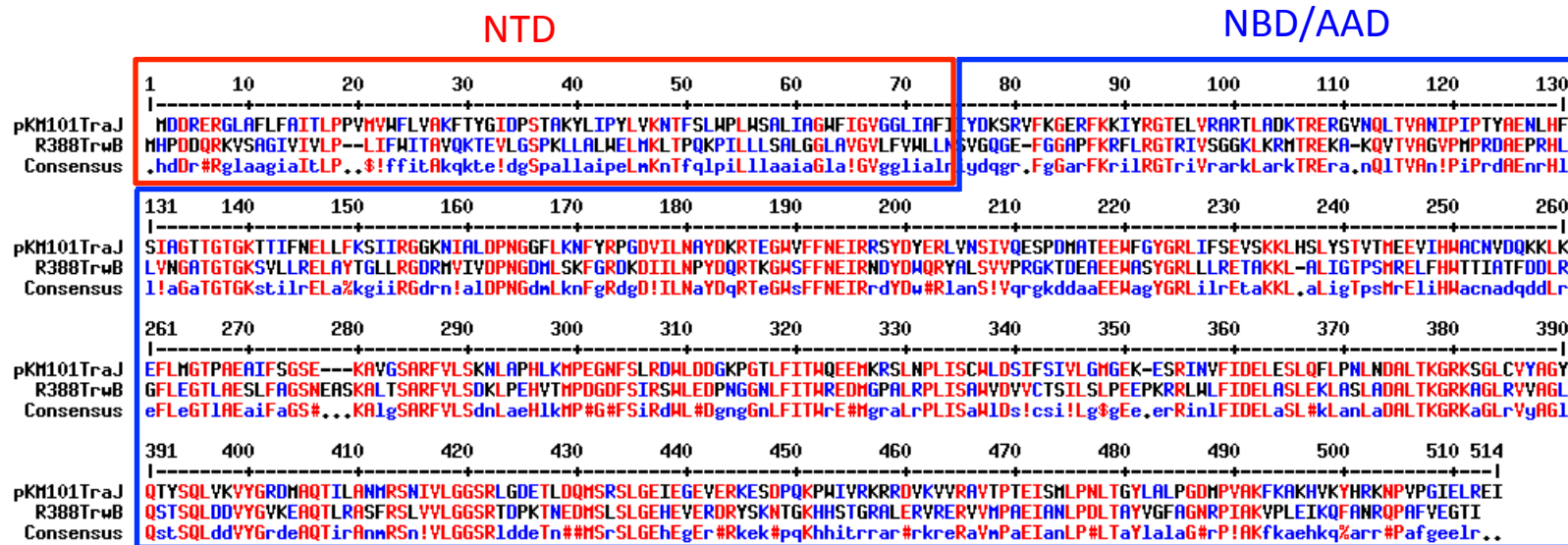


Fig. S2 Whitaker/Christie

C

Sequence Alignments of VirD4 Homologs

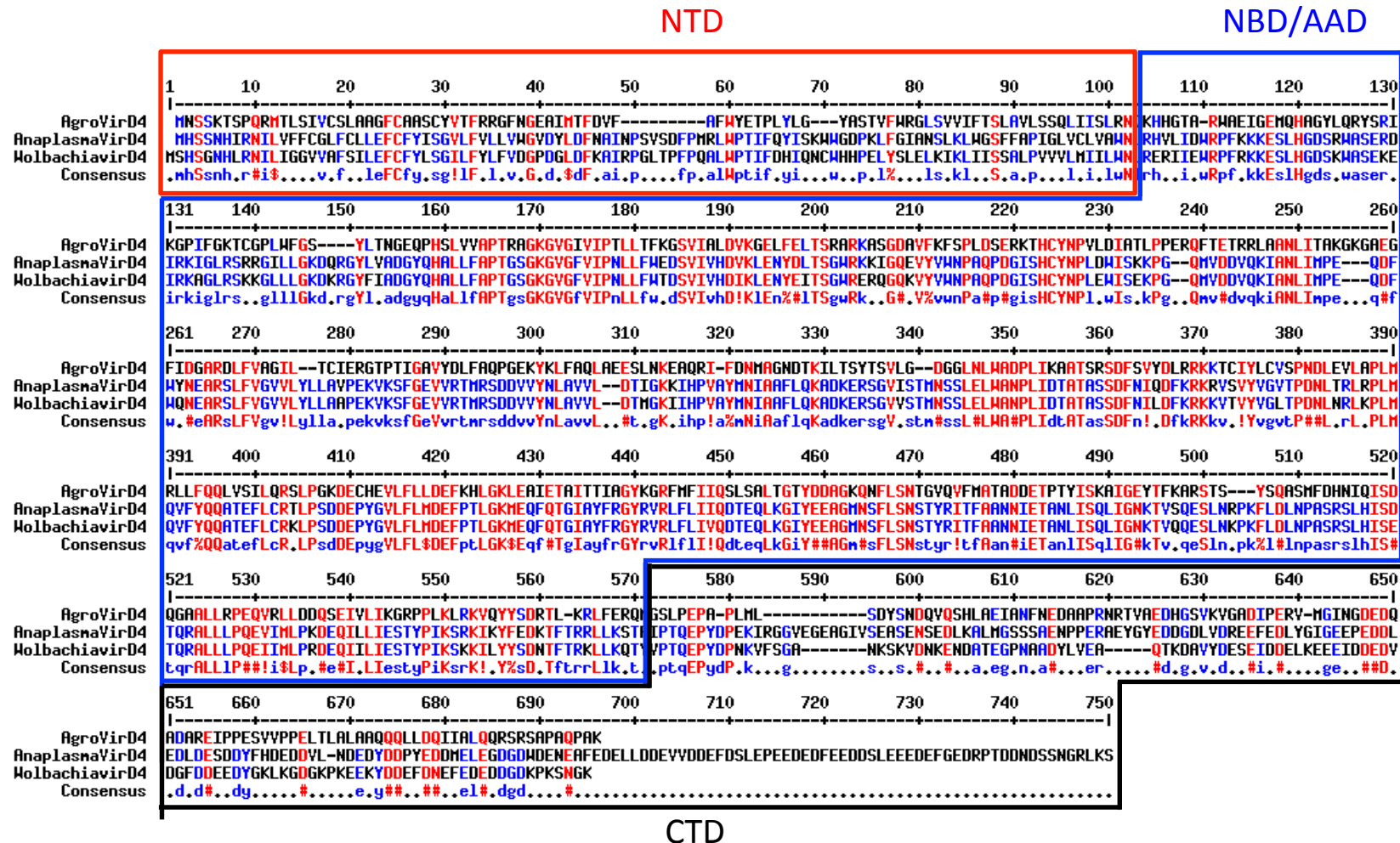


Fig. S2 Whitaker/Christie

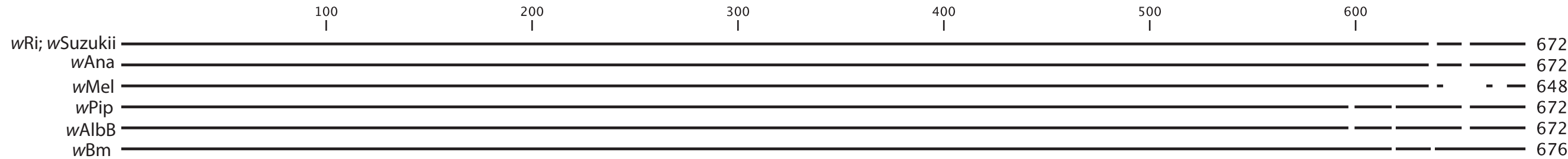
D

Sequence Alignments of VirD4 Homologs

Fig. S2 Whitaker/Christie

E (A)

CTD



(B)

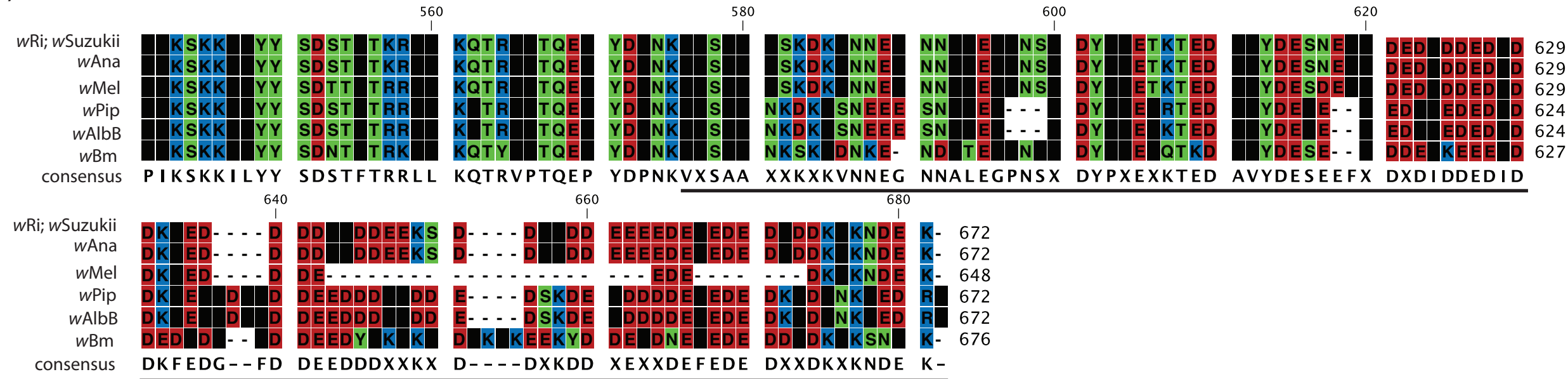


Fig. S2 Christie/Whitaker

		Charge	pI
VirE2	RLPADAAAGVLGEAADKYSRDFVRPEPASRPISDSRRIYESRPRSOSVNSF	+2	9.98
VirE3	DYHLSASEQENLLNOLLSPVPLPIPSPKPKSARSMIFEGSRPRERSTSRGF	+2.1	10.25
VirF	NVAEPIMFNEISALEVMAEVRIPIARSIKTAHDDRAELMSADRPRSTRGL	-0.9	5.54
Ats-1	AAMOOAVLSAARGLSDVSHDDSAOTQGNPTVTPLVSAONRGPETHGKGTR	+0.2	8.01
WD0636	IIVEELVKAGAEIEQADKFGMTAMDYAKNSKEVTEVKKETDRIEKLFEKL	-3.0	4.54
WD0811	TASKRTEQPKNDAPKKAGEPENNHHSTLFEQIRGGTTLKRVGSNKILQMN	+4.1	10.65
WalE1	SSTLTTRKQVLPLKEEFDRLEEKLAKR LASLDOPSAEPVNSRATATPGTV	0	6.99

Fig. S3 Whitaker/Christie

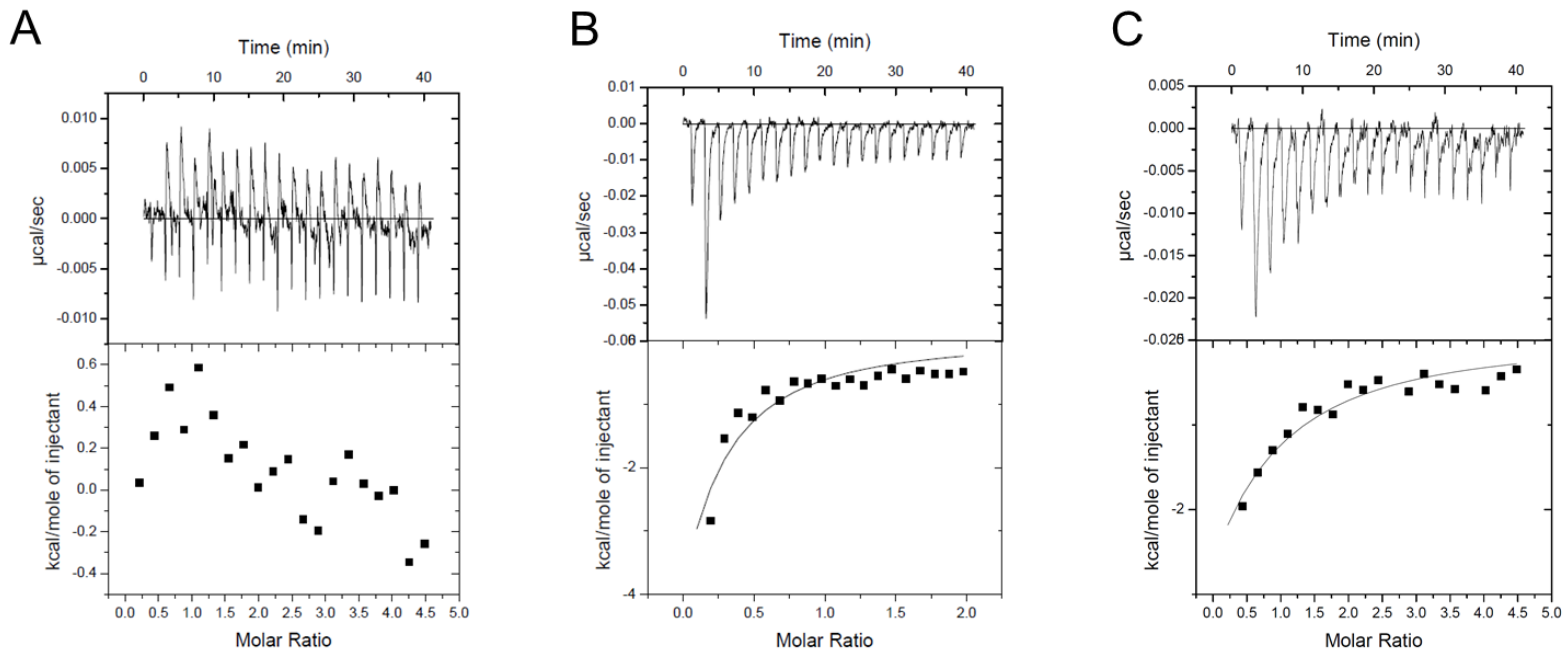


Fig S4. Whitaker/Christie